An Improved Boundary Integral Equation Method with Arbitrary Lagrangian-Eulerian Approach for Nonlinear Wave-Bottom Interaction Problems

Department of Civil & Environmental Engineering

Center for Computation & Technology

Wen-Huai Tsao[1,2] and Chris Kees[1,2]

[1]Department of Civil and Environmental Engineering, Louisiana State University, Baton Rouge, LA; [2]Center for Computation and Technology, Louisiana State University, Baton Rouge, LA;

Introduction

The goal of this study is to develop a fast and high-fidelity computational method for solving practical problems of physical oceanography, marine hydrodynamics, and ocean and coastal engineering. The application of the Arbitrary Lagrangian-Eulerian (ALE) method on a newly developed Regularized Boundary Integral Method (RBIM) for simulating water waves with topography based on fully nonlinear potential theory is presented. The RBIM is a meshless method for solving 2D and 3D potential flows [1,2]. The "subtraction and addition" technique is applied with compensatory integrals calculated through the coordinate transformation to regularize the boundary integral equation before implementing the numerical quadrature. Therefore, any high-order quadrature can be directly applied as collocation nodes without spatial discretization. Through the same technique, the numerical near-singularities of the source and doublet integrals can be handled to further improve the numerical accuracy. Chen et al. [3] attempted to solve the sloshing problem by RBIM in the classic Mixed Eulerian-Lagrangian (MEL) frame. Their MEL approach didn't cause any distortion of the element because the stochastic oscillatory wave inherently alleviates the large nodal shift. While as waves enter the complex topography, high nonlinearity and wave steeping will harm the numerical stability. The ALE handles the time derivatives in the third frame in addition to the Eulerian and Lagrangian frames. This method not only avoids distortion of the element but also keeps the convenience of the implementing free-surface boundary conditions. Therefore, the time-marching process remains robust. The numerical method is validated through two examples shown in Fig. 1.

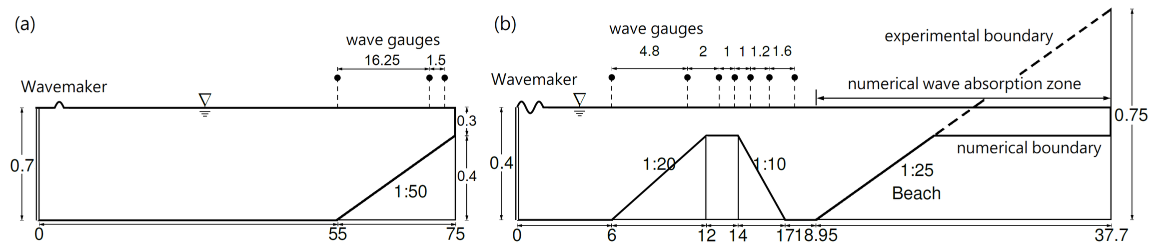

Fig. 1. The experimental and numerical configurations of (a) a solitary wave runs up a slope and reflect from a vertical wall (Walkley, 1999), (b) the periodic waves propagate over a submerged obstacle (Beji and Battjes, 1994).

Prior Work and Challenges

The potential-flow model is regarded as the balanced solution to wave problems. However, for large domains, such as rivers and oceans, developing a fast and robust solver is still an urgent task. This method will be implemented by the open-source computational toolkit *Proteus* (https://proteustoolkit.org/). *Proteus* can solve various practical problems in coastal, marine, and riverine environments through built-in FE and BE solvers for 2D and 3D flow and transport models, including the multi-phase RANS model, and dispersive shallow-water model. *Proteus* is also compatible with multi-body dynamic solver *Chrono*.

Potential Flow in Wave Problems

In potential flow, the fluid motion is governed by Laplace's equation expressed as:

$$\nabla^2\phi = 0 \tag{1}$$

where ϕ is the velocity potential. The kinematic, dynamic, impermeable, and radiation boundary conditions are applied on different fluid boundaries as:

$$\frac{D\boldsymbol{x}}{Dt} = \nabla\phi, on\, the\, free\, surface \tag{2}$$

$$\frac{D\phi}{Dt} = \frac{1}{2}|\nabla\phi|^2 - g\eta, on\, the\, free\, surface \tag{3}$$

$$\frac{\partial\phi}{\partial n} = \dot{\boldsymbol{x}}\cdot\boldsymbol{n}, on\, the\, wetted\, wall \tag{4}$$

$$\frac{\partial\phi}{\partial n} = -\frac{1}{c}\frac{\partial\phi}{\partial t}, on\, the\, outlet \tag{5}$$

where η is the wave elevation, n is the unit outward normal vector, and c is the celerity.

Regularized Boundary Integral Method

By applying Green's second identity to Green's function G and velocity potential ϕ, the BIE can be obtained as:

$$\int_S(\phi_q - \phi_p)\frac{\partial G(p,q)}{\partial n}dS = \int_S G(p,q)\frac{\partial\phi_q}{\partial n}dS \tag{6}$$

where $G(p,q) = lnr/2\pi$ is the 2D fundamental solution of Laplace's equation. Assume the load point p locates on a piecewise continuous boundary S_j shown in Fig. 2(a), the subtraction and addition technique can be applied to regularize the source integral as:

$$\int_{S_j} G(p,q)\frac{\partial\phi_q}{\partial n}dS = \int_0^L[G(p,q)\frac{\partial\phi_q}{\partial n}\frac{dS}{dx} - \frac{ln|x-x_p|}{2\pi}]dx + \frac{1}{2\pi}\frac{\partial\phi_p}{\partial n}\frac{dS_p}{dx}I_c \tag{7}$$

where I_c is the compensatory integral computed by:

$$I_c = \int_0^L ln|x-x_p|dx = (L-x_p)ln(x-x_p) + x_p ln x_p - L \tag{8}$$

Assume a load point p is not located on but very close to a piece-wise continuous boundary S_j shown in Fig. 2(b), the nearly singular integrals occur due to an insufficient number of numerical quadrature applied on the boundary. The subtraction and addition technique can be applied to remove the nearly singular integral of a doublet as:

$$\int_{S_j}\frac{\partial G(p,q)}{\partial n}\phi_q dS = \int_{S_j}\frac{\partial G(p,q)}{\partial n}(\phi_q - \phi_{q'})dS - \frac{\beta_1}{2\pi}\phi_{q'} \tag{9}$$

where q' is the closest collocation point to p on S_j. The nearly singular integral of a source can be removed as:

$$\int_{S_j} G(p,q)\frac{\partial\phi_q}{\partial n}dS = \int_0^L[G(p,q)\frac{\partial\phi_q}{\partial n} - \frac{1}{2\pi}ln\tau(\boldsymbol{n'_q}\cdot\boldsymbol{n})\frac{\partial\phi_{q'}}{\partial n}]dS + \frac{1}{2\pi}\frac{\partial\phi_{q'}}{\partial n}\frac{dS_p}{dx}I_{cn} \tag{10}$$

where I_{cn} is the compensatory integral computed by:

$$I_{cn} = L_1 ln\sqrt{\epsilon^2+L_1^2} + L_2 ln\sqrt{\epsilon^2+L_2^2} - L + \epsilon\beta_2 \tag{11}$$

The BIE implemented by RBIM can be rewritten in matrix form as:

$$\mathbf{A}\{\phi\} = \mathbf{B}\{\frac{\partial\phi}{\partial n}\} \tag{12}$$

Since the potential is given on the free surface and its normal derivative is given on the wetted boundaries, a mixed-type boundary value problem arises.

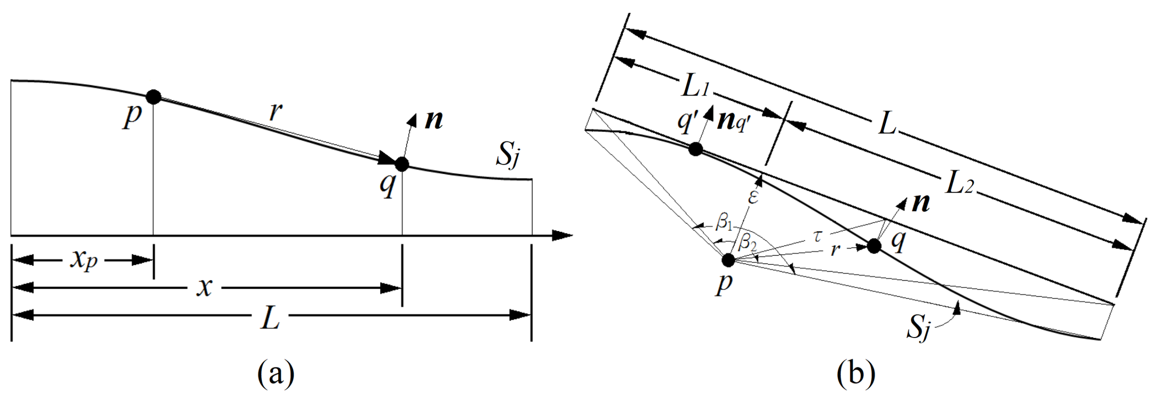

Fig. 2. The piecewise continuous boundary has (a) a source on it causing a singular integral, which can be solved by Eq. (7), (b) a source very close to it causing nearly singular integrals, which can be solved by Eqs. (9) and (10).

Arbitrary Lagrangian-Eulerian Method

In the ALE approach, the free surface is updated by the time derivatives handled in the third coordinate system χ as:

$$\boldsymbol{x}(t+\Delta t) = \boldsymbol{x}(t) + \Delta t\frac{d\boldsymbol{x}}{dt}|_\chi \tag{13}$$

$$\phi(t+\Delta t) = \phi(t) + \Delta t\frac{d\phi}{dt}|_\chi \tag{14}$$

where $\frac{d}{dt}|_\chi$ is the derivative operator in the ALE domain. Assuming the nodes of the rezoned mesh are on the same free surface as the Lagrangian nodes, and the reference frame is chosen so that the material velocity u and mesh velocity $\tilde{\boldsymbol{u}}$ have the same normal component, i.e., $\boldsymbol{u}\cdot\boldsymbol{n} = \tilde{\boldsymbol{u}}\cdot\boldsymbol{n}$. Hence,

$$\frac{dx_1}{dt}|_\chi = \tilde{u}_1 = 0 \tag{15}$$

$$\frac{dx_2}{dt}|_\chi = \tilde{u}_2 = u_2 + (u_1 - \tilde{u}_1)\frac{n_1}{n_2} \tag{16}$$

The time derivative of potential in the ALE frame is computed by:

$$\frac{d\phi}{dt}|_\chi = \frac{D\phi}{Dt} - \boldsymbol{c}\cdot\nabla\phi \tag{17}$$

Eqs. (13) and (14) will be used to implement the RK4 method for time integration.

Run-Up and Reflection of a Solitary Wave

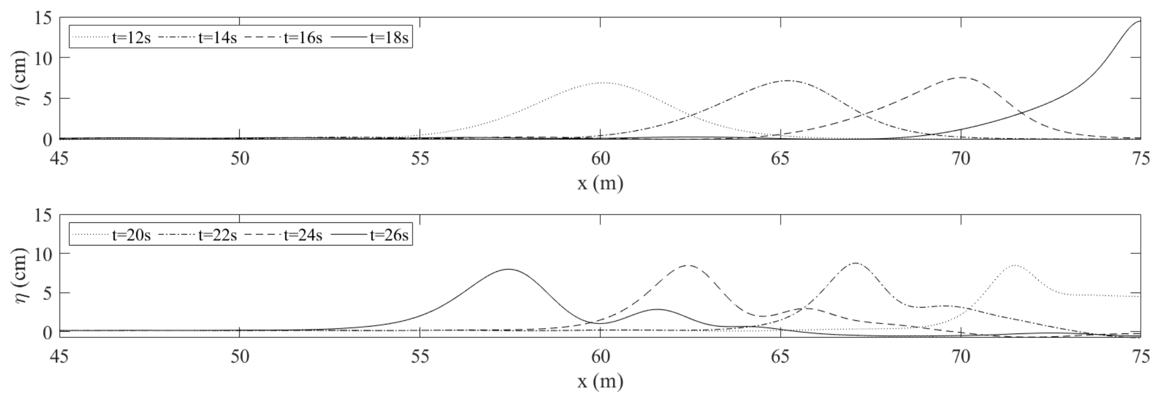

Fig. 3. The wave patterns of a solitary wave running up a slope and reflecting from the wall. The shoaling phenomenon is observed as the wave becomes steep as it propagates to the slope. As reflection begins, the water accumulates so the wave elevation on the wall is higher than the static water level. The reflected wave separated into one major wave followed by several minor ones.

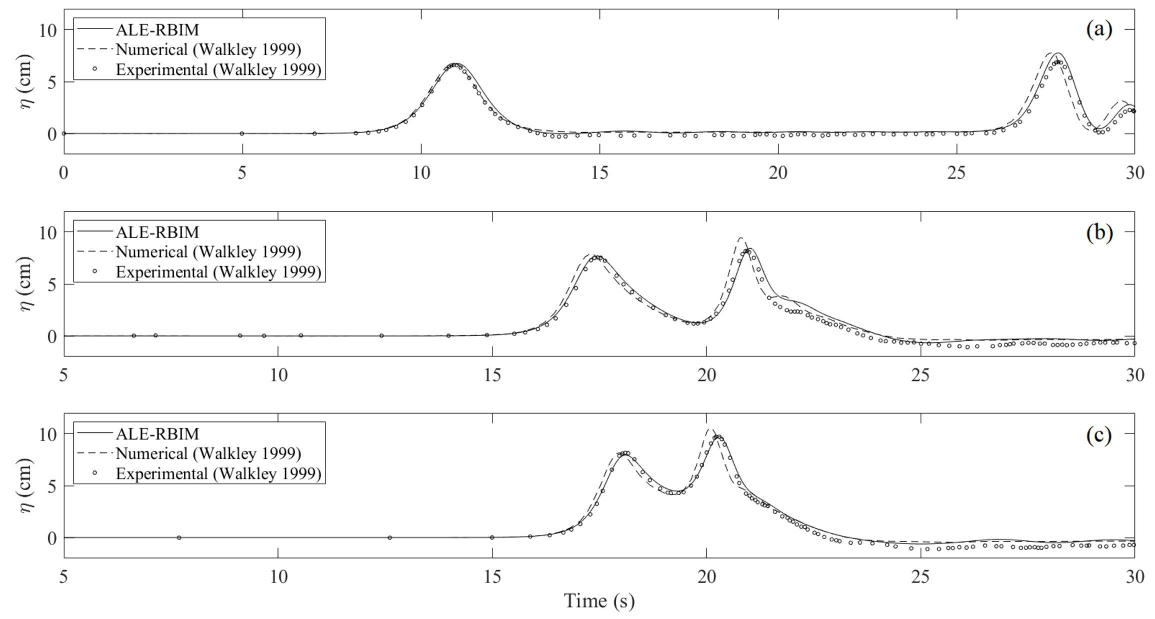

Fig. 4. The wave elevations in the test case of a solitary wave running up a slope and reflecting from the wall at (a) x = 55 m, (b) x = 71.25 m, (c) x = 72.75 m. The first and second peaks shown in the time history correspond to the incident wave and reflected wave, respectively. The present method captures the amplitudes and phases of both peaks precisely. Only a slight overshoot is obtained at the second peak of the reflected wave at x = 55 m because the potential-flow model wasn't able to describe the wave decay.

Periodic Waves Pass a Submerged Obstacle

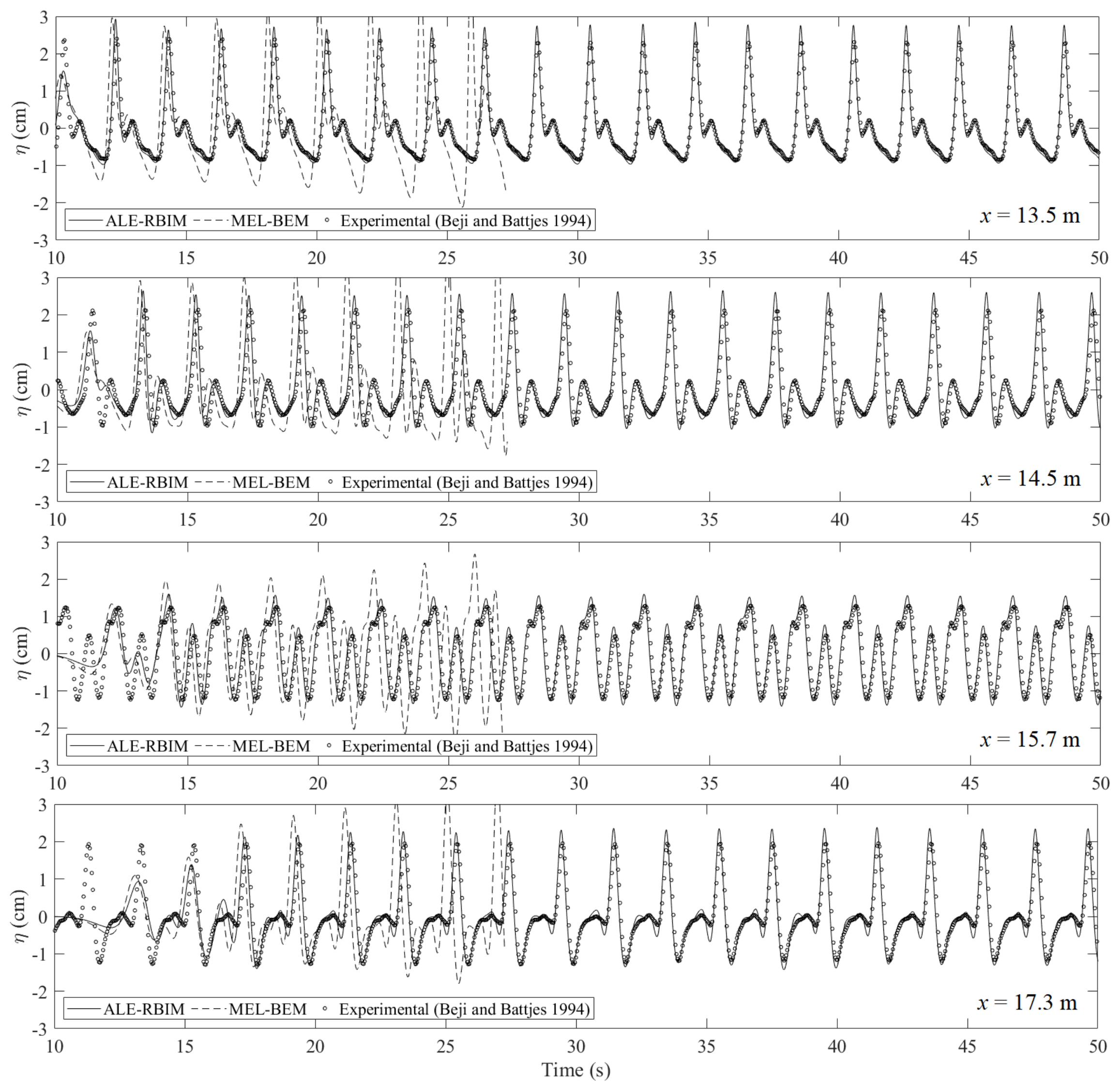

Fig. 5. The steady-state numerical and experimental wave elevations at the locations of the wave gauges. The results by ALE-RBIM are in good agreement with the experimental results. As higher harmonics are released behind the submerged bar, the present method remains very robust. The present method works better than the classic MEL-BEM, which can be unstable easily due to false velocity. This phenomenon can be explained by the free-surface elements shown in the following figures.

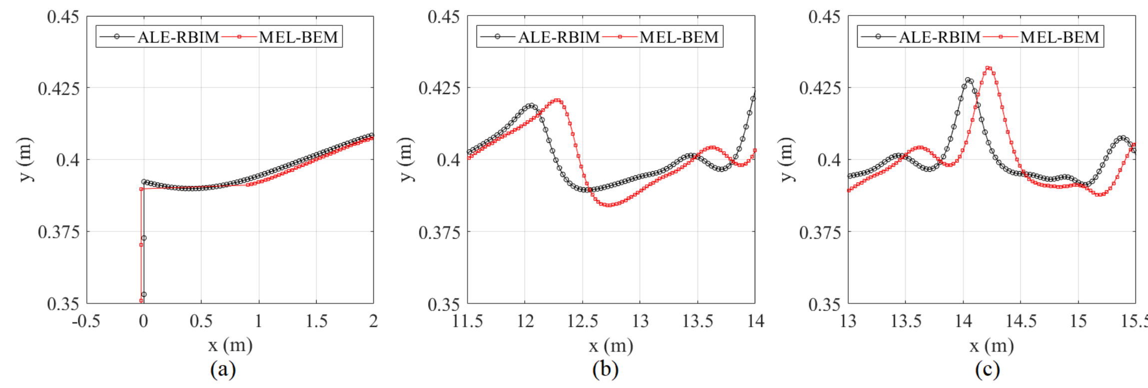

Fig. 6. The local wave patterns at t = 17 s given by ALE-RBIM and MEL-BEM. A large free-surface element near the wavemaker is obtained by MEL-BEM as shown in Fig. 6(a). Such distorted element enhances the discontinuity of the boundary and harms the accuracy of the numerical integration, hence resulting in large errors of nodal velocity. Therefore, the discrepancy appears in phase and amplitude as shown in Figs. 6(b) and 6(c). ALE method keeps equal spacing between collocation nodes to ensure the smoothness of the geometry. Therefore, no extra smoothing techniques for the free surface is needed. This allows the higher capability in simulating the high-order nonlinear waves that are more pronounced behind the submerged obstacle.

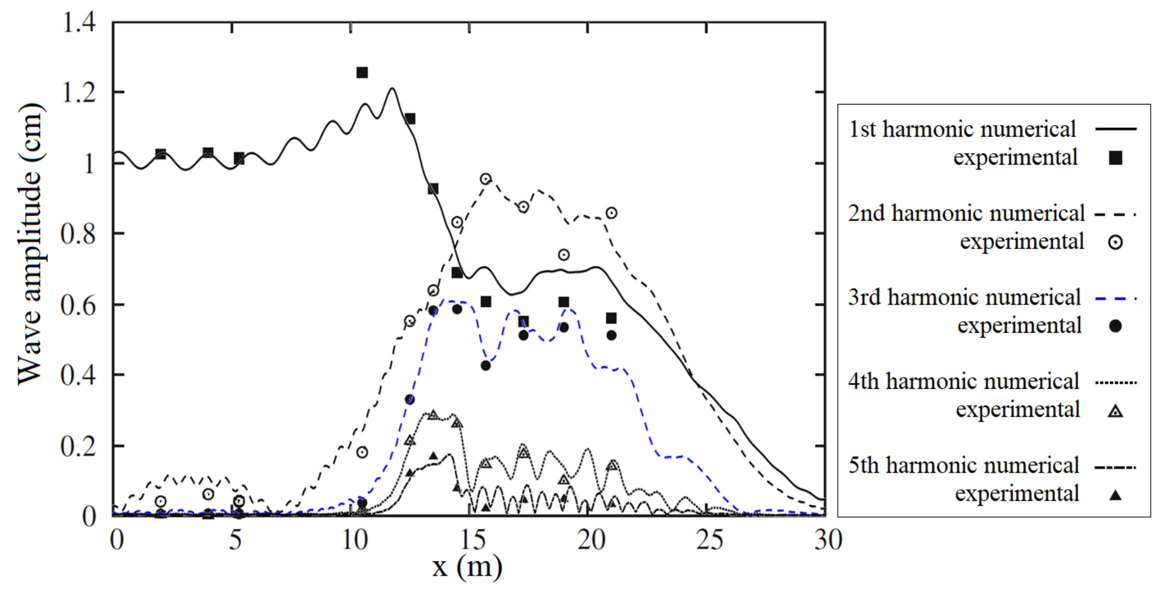

Fig. 7. The experimental and numerical steady-state wave amplitude of the first five harmonic components of the wave elevations for different locations. The incident wave is simple harmonic and regular. Within the slope area (6m≤x≤12m), the wave decomposition is well described and the highly dispersive characteristic is captured. When the waves pass over the shallowest zone (12m≤x≤14m), the second harmonic dominates. Finally, all components vanish due to the absorption condition. The present method is accurate in predicting the wave amplitudes, even for the smallest components that come from the highest fourth and fifth harmonics.

Future Work

The present study has shown the benefits of ALE-RBIM. Future works will emphasize the implementation of the Fast Multipole Method (FMM) in parallel ALE-RBIM to maximize numerical efficiency. We endeavor to provide a fast and reliable computational tool for large-scale 3D problems in coastal and ocean engineering.

References

[1] Hwang, W.S., Hung, L.P., and Ko, C.H. (2002). Non-singular boundary integral formulations for plane interior potential problems. *International Journal for Numerical Methods in Engineering*, 53:1751-1762.

[2] Tsao, W.H. and Hwang, W.S. (2017). Regularized boundary integral methods for three–dimensional potential flows. *Engineering Analysis with Boundary Elements*, 77:49-60.

[3] Chen, Y.H., Hwang, W.S. and Tsao, W.H. (2017). Nonlinear sloshing analysis by regularized boundary integral method. *Journal of Engineering Mechanics*, 143(8):40170046.